Journal of the Optical Society of Korea
Vol. 14, No. 3, September 2010, pp. 228-234
DOI: 10.3807/JOSK.2010.14.3.228

Joint-characteristic Function of the First- and Second-order Polarization-mode-dispersion Vectors in Linearly Birefringent Optical Fibers

Jae Seung Lee*

Department of Electronic Engineering, Kwangwoon University, 447-1 Wolgye-dong, Nowon-gu, Seoul 139-701, Korea

(Received June 28, 2010 : revised August 23, 2010 : accepted August 23, 2010)

This paper presents the joint characteristic function of the first- and second-order polarization-mode-dispersion (PMD) vectors in installed optical fibers that are almost linearly birefringent. The joint characteristic function is a Fourier transform of the joint probability density function of these PMD vectors. We regard the random fiber birefringence components as white Gaussian processes and use a Fokker-Planck method. In the limit of a large transmission distance, our joint characteristic function agrees with the previous joint characteristic function obtained for highly birefringent fibers. However, their differences can be noticeable for practical transmission distances.

Keywords : Polarization mode dispersion, Optical fiber, Optical fiber transmission, Optical communication
OCIS codes : (060.2300) Fiber measurements; (060.2330) Fiber optics communications; (060.2400) Fiber properties; (060.0060) Fiber optics and optical communications; (060.4510) Optical communications

I. INTRODUCTION

Random fluctuations of fiber birefringences cause polarization-mode dispersion (PMD) effects detrimental to high bit-rate channels. The PMD effects can be described using a PMD vector whose magnitude is equal to the differential group delay between two principal states [1], [2]. When there are many optical channels or the channel bit rate is high, the angular frequency derivative of the PMD vector becomes also important [3]. Often, the conventional PMD vector is called the first-order PMD vector while its angular frequency derivative is called the second-order PMD vector.

In [4], Foschini and Shepp derived a joint characteristic function for two white Gaussian vector processes in a compact functional form using a sine-cosine Fourier expansion representation. The joint characteristic function is a Fourier transform of the joint probability density function (pdf) of two vector processes. Shortly after [4], it was shown that, when the fiber transmission distance is large, the joint characteristic function can be used for the first- and second-order PMD vectors in highly birefringent fibers [5]. This joint characteristic function has been used extensively to describe various distribution characteristics of PMD vectors [6-8]. The birefringence vector model used in [5] assumes a fixed linear birefringence with much smaller linear and circular random birefringences in equal amounts. Interestingly, the joint characteristic function of [5] agrees with the result of [9] that uses the model of [5] without the fixed linear birefringence component. However, installed optical fibers are almost linearly birefringent [10]. Thus it is worthwhile to justify the joint characteristic function of [5] for installed fibers.

Regarding the birefringence components as white Gaussian processes, a Fokker-Planck equation [11] was derived in [12] to investigate the pdf behavior of the first-order PMD vector in linearly birefringent fibers. The Fokker-Planck method was used also in [13] to find a more correct joint characteristic function for the birefringence vector model of [9]. The second-order angular frequency derivative of the fiber birefringence vector was included in [13] but was neglected in [5] and [9]. The birefringence vector distribution of [9] and [13], having linear and circular random birefringences in equal amounts, has a spherical symmetry in Poincare space. This symmetry helps to find the joint characteristic functions of [9] and [13] that are dependent

*Corresponding author: jslee@kw.ac.kr

only on the magnitude of two PMD vectors and the angle in between in their Fourier domain. However, the spherical symmetry does not hold for installed optical fibers and, to our knowledge, the joint characteristic function for installed optical fibers is still unknown.

In this paper, we find the joint characteristic function for installed optical fibers. We use the Fokker-Planck method and include the second-order angular frequency derivative of the fiber birefringence vector. Our final result obtained after a complicated procedure has a compact functional form similar to the previous joint characteristic functions [5, 9, 13].

At first, we will present details of the Fokker-Planck method of [12] along with a new shortcut procedure for finding the pdf of the first-order PMD vector. Then we extend the approach to find a Fokker-Planck equation (in Fourier domain) for the first- and second-order PMD vectors. The asymptotic solution of our Fokker-Planck equation yields the joint characteristic function.

II. PDF FOR THE FIRST-ORDER PMD VECTOR

The dynamical PMD equation,

$$\frac{\partial \boldsymbol{\tau}}{\partial L} = \boldsymbol{\beta} \times \boldsymbol{\tau} + \boldsymbol{\beta}_\omega \tag{1}$$

describes the evolution of the first-order PMD vector, $\tau = (\tau_1, \tau_2, \tau_3)$ along the fiber [1]. L is the fiber transmission distance. $\boldsymbol{\beta}$ is the birefringence vector and $\boldsymbol{\beta}_\omega = \partial \boldsymbol{\beta} / \partial \omega$, where ω is the angular frequency. For linearly birefringent fibers, we set $\boldsymbol{\beta} = a(\Gamma_1, \Gamma_2, 0)$, where $\Gamma_i = \Gamma_i(L)$ (i=1, 2) is a zero-mean white Gaussian process having a correlation property, $E\{\Gamma_i(L)\Gamma_j(L')\} = 2\delta_{ij}\delta(L-L')$. $E\{\cdot\}$ denotes the ensemble average and δ_{ij} is the Kronecker delta. This modeling neglects the spatial size of the correlation length compared with the large parameter L [9], [12], [13]. The proportionality factor a is a function of ω and we will denote $da/d\omega$ as a_ω. Similarly, $d\boldsymbol{\beta}/d\omega$ is simplified to $\boldsymbol{\beta}_\omega = a_\omega(\Gamma_1, \Gamma_2, 0)$, etc.

We note that the vector equation (1) is composed of three Langevin equations, $\partial \tau_i / \partial L = \sum_{j=1}^{N} g_{ij}\Gamma_j$ (i=1, 2, 3), where N(=3) is the number of variables. The matrix formed by g_{ij} is

$$(g_{ij}) = \begin{pmatrix} a_\omega & a\tau_3 & 0 \\ -a\tau_3 & a_\omega & 0 \\ a\tau_2 & -a\tau_1 & 0 \end{pmatrix} \tag{2}$$

Then we find the Fokker-Planck equation as follows [11]:

$$\frac{\partial P}{\partial L} = -\sum_{i=1}^{N} \frac{\partial}{\partial \tau_i} D_i P + \sum_{i,j=1}^{N} \frac{\partial}{\partial \tau_i}\frac{\partial}{\partial \tau_j} D_{ij} P \tag{3}$$

where D_i and D_{ij} are drift and diffusion coefficients, respectively, defined as $D_i = \sum_{k,j=1}^{N} g_{kj}\partial g_{ij}/\partial \tau_k$ and $D_{ij} = \sum_{k=1}^{N} g_{ik} g_{jk}$.

From these relations, we have $D_1 = -a^2\tau_1$, $D_2 = -a^2\tau_2$, $D_3 = -a^2\tau_3$, and

$$(D_{ij}) = \begin{pmatrix} a_\omega^2 + a^2\tau_3^2 & 0 & aa_\omega\tau_2 - a^2\tau_1\tau_3 \\ 0 & a_\omega^2 + a^2\tau_3^2 & -aa_\omega\tau_1 - a^2\tau_2\tau_3 \\ aa_\omega\tau_2 - a^2\tau_1\tau_3 & -aa_\omega\tau_1 - a^2\tau_2\tau_3 & a^2(\tau_1^2 + \tau_2^2) \end{pmatrix}. \tag{4}$$

$P = P(\boldsymbol{\tau}; L)$ is the pdf for $\boldsymbol{\tau}$. Since the input signal has experienced no PMD degradations, the initial condition is a Dirac delta function, $P(\boldsymbol{\tau}, 0) = \delta(\boldsymbol{\tau})$.

The Fokker- Planck equation for the first-order PMD vector is given by

$$\frac{\partial P}{\partial L} = KP(\boldsymbol{\tau}, L) \tag{5}$$

where

$$K = a^2\left\{\frac{\partial}{\partial \tau_1}\tau_1 + \frac{\partial}{\partial \tau_2}\tau_2 + (\tau_1^2 + \tau_2^2)\frac{\partial^2}{\partial \tau_3^2} + \tau_3^2\left(\frac{\partial^2}{\partial \tau_1^2} + \frac{\partial^2}{\partial \tau_2^2}\right) + 2\left(1 - \frac{\partial}{\partial \tau_1}\tau_1 - \frac{\partial}{\partial \tau_2}\tau_2\right)\frac{\partial}{\partial \tau_3}\tau_3\right\}$$
$$+ 2aa_\omega\left(\tau_2\frac{\partial}{\partial \tau_1} - \tau_1\frac{\partial}{\partial \tau_2}\right)\frac{\partial}{\partial \tau_3} + a_\omega^2\left(\frac{\partial^2}{\partial \tau_1^2} + \frac{\partial^2}{\partial \tau_2^2}\right). \tag{6}$$

As is shown in Fig. 1, we use a spherical coordinate using the following transform relations [14]:

$$\frac{\partial}{\partial \tau_1} = \sin\theta\cos\varphi\frac{\partial}{\partial \tau} + \cos\theta\cos\varphi\frac{\partial}{\tau\partial\theta} - \frac{\sin\varphi}{\tau\sin\theta}\frac{\partial}{\partial\varphi} \tag{7}$$

$$\frac{\partial}{\partial \tau_2} = \sin\theta\sin\varphi\frac{\partial}{\partial \tau} + \cos\theta\sin\varphi\frac{\partial}{\tau\partial\theta} + \frac{\cos\varphi}{\tau\sin\theta}\frac{\partial}{\partial\varphi} \tag{8}$$

$$\frac{\partial}{\partial \tau_3} = \cos\theta\frac{\partial}{\partial \tau} - \sin\theta\frac{\partial}{\tau\partial\theta} \tag{9}$$

The positive τ_3-axis is the polar axis. θ and φ are polar and azimuth angles, respectively. Since our problem is invariant to

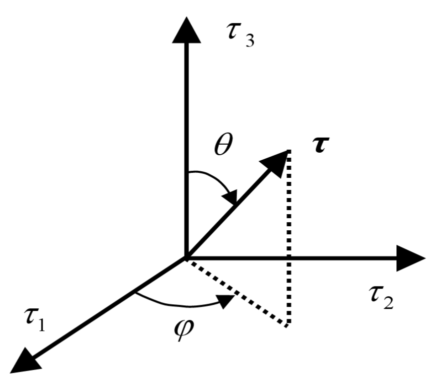

FIG. 1. Spherical coordinate for τ space.

the rotation about the τ_3-axis, we may set $\partial/\partial\varphi = 0$. Then the differential operator K can be simplified greatly as

$$K = a_\omega^2\left(\frac{\partial^2}{\partial\tau_1^2}+\frac{\partial^2}{\partial\tau_2^2}\right)+a^2\frac{1}{\sin\theta}\frac{\partial}{\partial\theta}\sin\theta\frac{\partial}{\partial\theta} \tag{10}$$

This equation implies that (5) is a diffusion equation along τ_1, τ_2, and θ directions. Therefore, in the asymptotic region, where the transmission distance L is large, $P=P(\boldsymbol{\tau}, L)$ becomes smooth and widely spread in $\boldsymbol{\tau}$ space.

We expand $P(\boldsymbol{\tau}, L)$ in terms of Legendre polynomials as $P(\boldsymbol{\tau}, L)=\sum_{n=0}^{\infty}A_n(\tau, L)P_n(\cos\theta)$. The n-th order Legendre polynomial, $P_n(\cos\theta)$, is an eigenmode of the a^2 term such that

$$\frac{1}{\sin\theta}\frac{\partial}{\partial\theta}\sin\theta\frac{\partial}{\partial\theta}P_n(\cos\theta) = -n(n+1)P_n(\cos\theta) \tag{11}$$

Since $P_n(\cos\theta)$ is not the eigenmode of a_ω^2 terms of (10), there are couplings between these modes during the transient region. The initial condition, $P(\boldsymbol{\tau}, 0)=\delta(\boldsymbol{\tau})$, belongs to the $P_0(\cos\theta)$ mode and $A_n(\tau, 0)$ for $n\neq0$. As L increases from zero, the magnitude of $A_n(\tau, L)$ $(n\neq0)$ increases owing to the coupling with the n=0 mode. Actually, these couplings exist only between even- modes owing to the even symmetry of our problem with respect to the θ coordinate. Note that the a^2 term in (10) is dependent only on the angular variable θ while the a_ω^2 terms are not. Thus, in the asymptotic region, where $P=P(\boldsymbol{\tau}, L)$ becomes smooth, the a^2 term becomes dominant compared with the a_ω^2 terms for $n\neq0$ modes. If a_ω^2 terms are neglected, $A_n(\tau, L)$ decays in proportion to $\exp\{-n(n+1)a^2L\}$. It implies that, in the asymptotic region, we have $P(\boldsymbol{\tau}, L)=A_0(\tau, L)$ ultimately. This can be verified also using a multiple-scale method [15].

To find $A_0(\tau, L)$ in the asymptotic region, we set $\partial/\partial\theta=\partial/\partial\varphi=0$ for the spherical coordinate representations of $\partial^2/\partial\tau_1^2$ and $\partial^2/\partial\tau_2^2$ terms in K, which gives

$$K = a_\omega^2\left\{\sin^2\theta\frac{\partial^2}{\partial\tau^2}+\left(\frac{1+\cos^2\theta}{\tau}\right)\frac{\partial}{\partial\tau}\right\}. \tag{12}$$

Next, we remove the terms in K that couple $A_0(\tau)$ with other $A_n(\tau, L)$ $(n\neq0)$ components. This can be achieved by applying $(1/2)\int_0^\pi d\theta\sin\theta$ on K, which leaves only the $P_0(\cos\theta)$ component in K. The result is

$$\frac{\partial P}{\partial L} = \frac{2}{3}a_\omega^2\left(\frac{\partial^2}{\partial\tau^2}+\frac{2}{\tau}\frac{\partial}{\partial\tau}\right)P. \tag{13}$$

Thus, in the asymptotic region, $P(\boldsymbol{\tau}, L)$ becomes a Gaussian, $\exp(-\tau^2/2\sigma^2)/(\sqrt{2\pi\sigma})^3$ with a variance $\sigma^2(L)=4a_\omega^2L/3$. This also implies that the magnitude of the first order PMD vector's pdf converges to a Maxwellian [2].

We have used the same initial condition, $P(\boldsymbol{\tau}, 0)=\delta(\boldsymbol{\tau})$, to solve (13). This can be verified by taking a Laplace transform of (5) to find $s\tilde{P}(\boldsymbol{\tau}, s)-\delta(\boldsymbol{\tau})=K\tilde{P}(\boldsymbol{\tau}, s)$, where $\tilde{P}(\boldsymbol{\tau}, s)$ is the Laplace transform of $\tilde{P}(\boldsymbol{\tau}, L)$ with respect to L. The initial condition term, $\delta(\boldsymbol{\tau})$, also belongs to the $P_0(\cos\theta)$ mode and remains the same in the asymptotic region. Thus the initial condition, $P(\boldsymbol{\tau}, 0)=\delta(\boldsymbol{\tau})$, can be used for (13).

III. JOINT CHARACTERISTIC FUNCTION FOR THE FIRST-AND SECOND-ORDER PMD VECTORS

From (1), we find a differential equation for the second-order PMD vector, $\boldsymbol{\tau}_\omega=\partial\boldsymbol{\tau}/\partial\omega=(\tau_{\omega1}, \tau_{\omega2}, \tau_{\omega3})$, as follows:

$$\frac{\partial\boldsymbol{\tau}_\omega}{\partial L} = \boldsymbol{\beta}_\omega\times\boldsymbol{\tau}+\boldsymbol{\beta}\times\boldsymbol{\tau}_\omega+\boldsymbol{\beta}_{\omega\omega} \tag{14}$$

where $\boldsymbol{\beta}_{\omega\omega}=\partial^2\boldsymbol{\beta}/\partial\omega^2=a_{\omega\omega}(\Gamma_1, \Gamma_1, 0)$. We note that (1) and (14) can be regarded as six Langevin equations, $\partial x_i/\partial L=\sum_{j=1}^{N}g_{ij}\Gamma_j$ where N=6. $x_i=\tau_i$ for i = 1, 2, 3 and $x_i=\tau_{\omega i}$ for i = 4, 5, 6. Now g_{ij} set forms a 6×6 matrix that will be used to find new drift and diffusion coefficients in the Fokker-Planck equation, (3). Its solution is the joint pdf of $\boldsymbol{\tau}$ and $\boldsymbol{\tau}_\omega$ which will be denoted as $P=P(\boldsymbol{\tau}, \boldsymbol{\tau}_\omega, L)$.

We will solve the Fokker-Planck equation in the Fourier domain by introducing a joint characteristic function,

$$Q(\boldsymbol{k},\boldsymbol{k}_\omega,L)=\iint d\boldsymbol{\tau}d\boldsymbol{\tau}_\omega\exp(-j\boldsymbol{k}\cdot\boldsymbol{\tau}-j\boldsymbol{k}_\omega\cdot\boldsymbol{\tau}_\omega)P(\boldsymbol{\tau},\boldsymbol{\tau}_\omega,L) \tag{15}$$

where $\boldsymbol{k}=(k_1, k_2, k_3)$ and $\boldsymbol{k}_\omega=(k_{\omega1}, k_{\omega2}, k_{\omega3})$. Our definition of the join]t characteristic function is the complex conjugate of the conventional one. The differential equation for the joint characteristic function is given as

$$\frac{\partial Q(\boldsymbol{k},\boldsymbol{k}_\omega,L)}{\partial L} = MQ(\boldsymbol{k},\boldsymbol{k}_\omega,L) \tag{16}$$

where the differential operator M is given by

$$M=a^2A+a_\omega^2B+a_{\omega\omega}^2C+2aa_\omega D+2a_\omega a_{\omega\omega}E+2aa_{\omega\omega}F \tag{17}$$

$$A=(\boldsymbol{k}\times\nabla_{\boldsymbol{k}}+\boldsymbol{k}_\omega\times\nabla_{\boldsymbol{k}_\omega})^2=-(\boldsymbol{L}_{\boldsymbol{k}}+\boldsymbol{L}_{\boldsymbol{k}_\omega})^2=-\boldsymbol{L}_{tot}^2 \tag{18}$$

$$B=(k_{\omega2}\partial/\partial k_3-k_{\omega3}\partial/\partial k_2+jk_1)^2+(k_{\omega3}\partial/\partial k_1-k_{\omega1}\partial/\partial k_3+jk_2)^2 \tag{19}$$

$$C=-(k_{\omega1}^2+k_{\omega2}^2) \tag{20}$$

$$\begin{aligned}D=k_3L_{k3}-k_2L_{k\omega2}-k_1L_{k\omega1}+(jk_{\omega2}\partial/\partial k_3-jk_{\omega3}\partial/\partial k_2\\-k_{\omega3}\partial/\partial k_1+k_{\omega1}\partial/\partial k_3)L_{tot-}/2+(jk_{\omega2}\partial/\partial k_3-jk_{\omega3}\partial/\partial k_2\\+k_{\omega3}\partial/\partial k_1-k_{\omega1}\partial/\partial k_3)L_{tot+}/2\end{aligned} \tag{21}$$

$$E = -k_1 k_{\omega 1} - k_2 k_{\omega 2} - jk_{\omega 1} k_{\omega 3} \partial / \partial k_2 + jk_{\omega 2} k_{\omega 3} \partial / \partial k_1 \quad (22)$$

$$F = k_{\omega 3} L_{k\omega 3} - k_{\omega 2} L_{k2} - k_{\omega 1} L_{k1} \quad (23)$$

In (18), we have introduced angular momentum operators defined as $\boldsymbol{L_k} = -j\boldsymbol{k} \times \nabla_{\boldsymbol{k}} = (L_{k1}, L_{k2}, L_{k3})$, $\boldsymbol{L_{k\omega}} = -j\boldsymbol{k_\omega} \times \nabla_{\boldsymbol{k\omega}} = (L_{k\omega 1}, L_{k\omega 2}, L_{k\omega 3})$, and $\boldsymbol{L_{tot}} = \boldsymbol{L_k} + \boldsymbol{L_{k\omega}} = (L_{tot1}, L_{tot2}, L_{tot3})$ [16]. $\nabla_{\boldsymbol{k}}$ and $\nabla_{\boldsymbol{k\omega}}$ are del operators in $\boldsymbol{k}$ and $\boldsymbol{k_\omega}$ domains, respectively. $L_{tot+} = L_{tot1} + jL_{tot2}$ and $L_{tot-} = L_{tot1} - jL_{tot2}$ are raising and lowering operators, respectively, for the total angular momentum operator, $\boldsymbol{L_{tot}}$. Since the input signal has experienced no PMD degradations, the initial condition is $Q(\boldsymbol{k}, \boldsymbol{k_\omega}, 0) = 1$ or $P(\boldsymbol{\tau}, \boldsymbol{\tau_\omega}, 0) = \delta(\boldsymbol{\tau})\delta(\boldsymbol{\tau_\omega})$.

As is shown in the Appendix A, we can find $E\{\tau^2\} = 4a_\omega^2 L$ from (16) using the relation, $E\{\tau^2\} = -\nabla_k^2 Q(\boldsymbol{k}, \boldsymbol{k_\omega}, L)|_{\boldsymbol{k}=\boldsymbol{k_\omega}=0}$. In a similar way, $E\{\tau_\omega^2\}$ is found as $16a_\omega^4 L^2/3 + 4a_{\omega\omega}^2 L(1 - a_\omega^4 / 9a_{\omega\omega}^2 a^2) + 2a_\omega^4\{1 - \exp(-6a^2 L)\}/27a^4$. As L becomes large, the ratio $E\{\tau_\omega^2\}/(E\{\tau^2\})^2$ converges to 1/3 [5]. In this asymptotic region, $Q(\boldsymbol{k}, \boldsymbol{k_\omega}, L)$ becomes localized to the origin $\boldsymbol{k}=\boldsymbol{k_\omega}=0$.

Since $E\{\tau_\omega^2\} >> E\{\tau^2\}$, $Q(\boldsymbol{k}, \boldsymbol{k_\omega}, L)$ shrinks faster in $\boldsymbol{k_\omega}$ domain than in $\boldsymbol{k}$ domain as L increases.

The $\boldsymbol{L}_{tot}^2$ operator has eigenvalue $L_{tot}(L_{tot}+1)$, where L_{tot} is a non-negative integer. We may expand $Q(\boldsymbol{k}, \boldsymbol{k_\omega}, L)$ using the eigenmodes of $\boldsymbol{L}_{tot}^2$. The $\boldsymbol{L}_{tot}^2$ operator is composed of angular variables only and becomes dominant in the asymptotic region. The other terms in M become less effective. This is because, as is mentioned above, $Q(\boldsymbol{k}, \boldsymbol{k_\omega}, L)$ shrinks to the origin $\boldsymbol{k}=\boldsymbol{k_\omega}=0$ and the shrink speed is faster in $\boldsymbol{k_\omega}$ domain. Thus eigenmodes with $L_{tot} \neq 0$ become negligible in the asymptotic region and only the eigenmode with $L_{tot} = 0$ survives. Note that this procedure is similar to the foregoing first-order PMD vector analysis. The $L_{tot} = 0$ condition also implies that the only possible eigenvalue of $L_{tot\,3}$ is zero since $-L_{tot} \le L_{tot3} \le L_{tot}$. Thus we have $L_{tot\pm} Q = L_{tot3} Q = 0$ or

$$\boldsymbol{L_{tot}} Q = -j(\boldsymbol{k} \times \nabla_{\boldsymbol{k}} + \boldsymbol{k_\omega} \times \nabla_{\boldsymbol{k\omega}}) Q = 0\,. \quad (24)$$

From (24), we find $\boldsymbol{k} \cdot \boldsymbol{L_{k\omega}} Q = \boldsymbol{k_\omega} \cdot \boldsymbol{L_k} Q = 0$. Using these relations, it can be shown that D and F terms in the operator M disappear, i.e., $DQ = FQ = 0$. As a result, there are no differential terms for $\boldsymbol{k_\omega}$ in the operator M and $\boldsymbol{k_\omega}$ becomes just a parameter in the asymptotic region. The symmetry in (24) implies that the asymptotic solution should be dependent only on the magnitudes of $\boldsymbol{k}$ and $\boldsymbol{k_\omega}$ vectors and the angle in between. This can be proved simply by rotating the coordinate such that one of $\boldsymbol{k}$ or $\boldsymbol{k_\omega}$ vector becomes a polar axis.

To find the asymptotic solution satisfying this condition, let's assume that the $\boldsymbol{k_\omega}$ vector is located in the $\boldsymbol{k}$ vector domain as is shown in Fig. 2. Since our problem is invariant under the rotation about the k_3-axis, we have set $k_{\omega 2}$. We rotate the (k_1, k_2, k_3) coordinate about the k_2 -axis

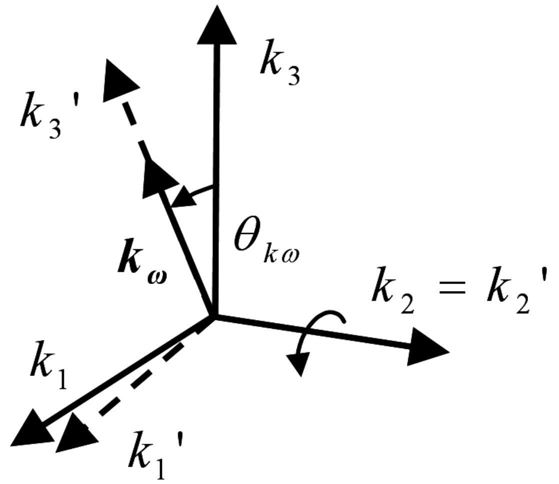

FIG. 2. Rotation of $\boldsymbol{k}$ vector space coordinates about the k_2 -axis.

into the (k_1', k_2', k_3') coordinate, where the k_3' -axis coincides with the $\boldsymbol{k_\omega}$ vector's direction.

The corresponding rotation matrix is

$$\boldsymbol{R}(\theta_{k\omega}) = \begin{pmatrix} \cos\theta_{k\omega} & 0 & -\sin\theta_{k\omega} \\ 0 & 1 & 0 \\ \sin\theta_{k\omega} & 0 & \cos\theta_{k\omega} \end{pmatrix}. \quad (25)$$

where $\theta_{k\omega}$ is the polar angle of k_ω before the rotation. With (25), we apply the transform relations $k_i = \sum_{j=1}^{3} R_{ji} k_j'$ and $\partial / \partial k_i = \sum_{j=1}^{3} R_{ji} \partial / \partial k_j'$ (i=1, 2, 3) to M, where R_{ji} is the matrix element of the inverse rotation matrix $R(-\theta_{k\omega})$. Then the remaining operators, B, C, and E, are transformed into

$$\begin{aligned} B = {} & k_\omega^2 \partial^2 / \partial k_1'^2 + k_\omega^2 \cos^2\theta_{k\omega} \partial^2 / \partial k_2'^2 \\ & - 2jk_\omega \cos\theta_{k\omega} (k_1' \cos\theta_{k\omega} + k_3' \sin\theta_{k\omega}) \partial / \partial k_2' \\ & - (k_1' \cos\theta_{k\omega} + k_3' \sin\theta_{k\omega})^2 - k_2'^2 + 2jk_\omega k_2' \partial / \partial k_1' \end{aligned} \quad (26)$$

$$C = -k_\omega^2 \sin^2\theta_{k\omega} \quad (27)$$

$$\begin{aligned} E = {} & -(k_1' \cos\theta_{k\omega} + k_3' \sin\theta_{k\omega}) k_\omega \sin\theta_{k\omega} \\ & - jk_\omega^2 \sin\theta_{k\omega} \cos\theta_{k\omega} \partial / \partial k_2' \end{aligned} \quad (28)$$

In the transformed (k_1', k_2', k_3') coordinate, the asymptotic solution is not dependent on the azimuth angle φ'. Thus we set $\partial / \partial \varphi' = k_1' \partial / \partial k_2' - k_2' \partial / \partial k_1' = 0$ in M. In addition, we apply $(1/4\pi)\int_0^\pi d\theta_{k\omega} \sin\theta_{k\omega} \int_0^{2\pi} d\varphi'$ on M to remove $\theta_{k\omega}$ and φ' dependences in M. This operation removes the couplings between the $L_{tot} = 0$ mode and the other modes with $L_{tot} \neq 0$. Then $\cos^2\theta_{k\omega}$, $\sin^2\theta_{k\omega}$, and $\sin\theta_{k\omega}\cos\theta_{k\omega}$ factors become 1/3, 2/3, and 0, respectively. Also, $\cos^2\varphi'$, $\sin^2\varphi'$, and $\sin\varphi'\cos\varphi'$ factors become 1/2, 1/2, and 0, respectively. Besides, we find $\partial / \partial k_1'^2 = \partial / \partial k_2'^2$.

Finally, we obtain the following differential equation for the asymptotic solution:

$$\frac{\partial Q}{\partial L} = \frac{2}{3}\left[a_\omega^2 \left\{ k_\omega^2 \left(\frac{\partial^2}{\partial k_1^2} + \frac{\partial^2}{\partial k_2^2} \right) - k^2 \right\} - (a_{\omega\omega}^2 k_\omega^2 + 2a_\omega a_{\omega\omega} k_3 k_\omega) \right] Q \tag{29}$$

where we have omitted the prime notation. As before, the initial condition remains the same, $Q(\boldsymbol{k}, \boldsymbol{k}_\omega, 0) = 1$. We decompose $Q(\boldsymbol{k}, \boldsymbol{k}_\omega, L)$ as

$$Q = \exp\left\{ -\left(a_\omega k_3 + a_{\omega\omega} k_\omega \right)^2 (2L/3) \right\} q(k_1, k_2, L) \tag{30}$$

where q satisfies

$$\frac{\partial q}{\partial L} = \frac{2}{3}\left\{ -a_\omega^2 \left(k_1^2 + k_2^2 \right) + a_\omega^2 k_\omega^2 \left(\frac{\partial^2}{\partial k_1^2} + \frac{\partial^2}{\partial k_2^2} \right) \right\} q . \tag{31}$$

Equation (31) can be solved using the separation-of-variables method as

$$\begin{aligned} q(k_1, k_2, L) = {} & 2\exp\left\{ -(k_1^2 + k_2^2)/2k_\omega \right\}. \\ & \cdot \sum_{m,n=0}^{\infty} \frac{\exp\left[-\{4(m+n)+2\} a_\omega^2 k_\omega (2L/3) \right]}{4^{m+n} m! n!} \\ & \cdot H_{2m}\left(k_1 / \sqrt{k_\omega} \right) H_{2n}\left(k_2 / \sqrt{k_\omega} \right) \end{aligned} \tag{32}$$

where $H_{2m}(\cdot)$ is the Hermite polynomial. Using an expansion formula for a Gaussian function,

$$\begin{aligned} \exp\left(-\frac{x^2}{2}\tanh y\right) = {} & \sqrt{\frac{2}{1+\tanh y}} \\ & \cdot \exp\left(-\frac{x^2}{2}\right) \sum_{m=0}^{\infty} \frac{\exp(-2my)}{4^m m!} H_{2m}(x) \end{aligned} \tag{33}$$

we find

$$q(k_1, k_2, L) = \frac{\exp\left\{ -\dfrac{k_1^2 + k_2^2}{2k_\omega} \tanh\left(4a_\omega^2 k_\omega L/3 \right) \right\}}{\cosh\left(4a_\omega^2 k_\omega L/3 \right)} . \tag{34}$$

Thus, for an arbitrary direction of $\boldsymbol{k}_\omega$, the joint characteristic function becomes

$$\begin{aligned} Q(\boldsymbol{k}, \boldsymbol{k}_\omega, L) = {} & \frac{\exp\left\{ -\dfrac{k_\perp^2}{2k_\omega} \tanh\left(k_\omega \sigma^2 \right) \right\}}{\cosh\left(k_\omega \sigma^2 \right)} \\ & \cdot \exp\left\{ -\left(a_\omega k_{//} + a_{\omega\omega} k_\omega \right)^2 (2L/3) \right\} \end{aligned} \tag{35}$$

where $\sigma^2 = E\{\tau_1^2\} = E\{\tau_2^2\} = E\{\tau_3^2\} = 4a_\omega^2 L/3$ as in the previous section. $\boldsymbol{k}_{//}$ is the component of $\boldsymbol{k}$ parallel to $\boldsymbol{k}_\omega$ and $k_\perp^2 = k^2 - k_{//}^2$.

In the limit of large L, the $\cosh\left(k_\omega \sigma^2 \right)$ term in (35) implies that the effective range of k_ω decreases as $O(L^{-1})$ since $\sigma^2 \propto L$. Also, the exponential terms in (35) imply that the effective range of $k_i (i=1, 2, 3)$ decreases as $O(L^{-1/2})$. Thus we may neglect the $a_{\omega\omega}$ term in (35) as L increases indefinitely. In this limit, (35) becomes the same as the joint characteristic function of [5] with reevaluated σ^2 appropriate to the linearly birefringent fiber. This feature also holds when the fiber has both linear and circular birefringences in equal amounts [9], [13]. The $a_{\omega\omega}$ term can be meaningful for practical transmission distances. For example, the second-order PMD vector components can be Gaussian-like distributed instead of a soliton shape [2]. This point has been shown in [13] and presented in Appendix B.

With the $\beta_3 = a\Gamma_3$ condition, the first-order PMD vector distribution has an azimuthal symmetry for all L in [12]. However, the azimuthal symmetry is not evident in our analysis of joint-characteristic function where the number of variables is doubled from 3 to 6. In fact, our final asymptotic solution (35) has spherical symmetry. The coordinate orientation does not affect our result. This kind of spherical symmetry for the asymptotic joint-characteristic function is also found in [5], [9], and [13].

It is also interesting that (35) is quite similar to the result of [13]. The only difference is the change of L into $2L/3$ in our case. In [13], the birefringence vector was assumed as $\boldsymbol{\beta} = a(\Gamma_1, \Gamma_2, \Gamma_3)$ where $\Gamma_3 = \Gamma_3(L)$ is also a zero-mean white Gaussian process having a correlation property, $E\{\Gamma_3(L)\,\Gamma_i(L')\} = 2\delta_{3i}\delta(L - L')$ for $i = 1, 2, 3$. Note that the number of random birefringence components is larger than our case. Thus, for given a, a_ω, and $a_{\omega\omega}$ values, the joint characteristic function reaches to its asymptotic form faster than our case as the transmission distance increases. In this respect, the scaling factor 2/3 can be regarded as the ratio of the birefringence component numbers.

IV. CONCLUSION

We have found a joint characteristic function for the first- and second-order PMD vectors in installed fibers. As the fiber transmission distance increases indefinitely, our joint characteristic function resembles that of [5] obtained for highly birefringent fibers. This agreement may not hold for practical transmission distances owing to the second-order angular frequency derivative of the fiber birefringence vector included in our analysis. As an example, we have shown that the second-order PMD vector components can be Gaussian-like distributed instead of a soliton shape. If the fiber length is scaled by a factor of 2/3, our result obtained for linearly birefringent fibers has the same functional form with the previous joint characteristic function of [13] obtained for fibers having a spherically symmetric birefringence vector distribution in Poincare space.

APPENDIX A

We derive $E\{\tau^2\}$ and $E\{\tau_\omega^2\}$ from the Fokker-Planck equation in the Fourier domain (16).

Since $Q(\boldsymbol{k},\boldsymbol{k}_\omega,L)=E\{\exp(-j\boldsymbol{k}\cdot\boldsymbol{\tau}-j\boldsymbol{k}_\omega\cdot\boldsymbol{\tau}_\omega)\}$, $E\{\tau_i^2\}$ (i=1, 2, 3) can be evaluated as

$$E\{\tau_i^2\}=-\left\{\frac{\partial^2}{\partial k_i^2}Q(\boldsymbol{k},\boldsymbol{k}_\omega,L)\right\}\Bigg|_{\boldsymbol{k}=\boldsymbol{k}_\omega=0}. \tag{A1}$$

Applying $\partial^2/\partial k_i^2$ to (16) and setting $\boldsymbol{k}=\boldsymbol{k}_\omega=0$, we find

$$\frac{\partial}{\partial L}E\{\tau_1^2\}=-2a^2\left(E\{\tau_1^2\}-E\{\tau_3^2\}\right)+2a_\omega^2. \tag{A2}$$

$$\frac{\partial}{\partial L}E\{\tau_2^2\}=-2a^2\left(E\{\tau_2^2\}-E\{\tau_3^2\}\right)+2a_\omega^2 \tag{A3}$$

$$\frac{\partial}{\partial L}E\{\tau_3^2\}=2a^2\left(E\{\tau_1^2\}+E\{\tau_2^2\}\right)-4a^2E\{\tau_3^2\} \tag{A4}$$

Adding these equations, we have

$$\frac{\partial}{\partial L}\left(E\{\tau_1^2\}+E\{\tau_2^2\}+E\{\tau_3^2\}\right)=\frac{\partial}{\partial L}E\{\tau^2\}=4a_\omega^2. \tag{A5}$$

Thus $E\{\tau^2\}=4a_\omega^2L$ for all L. Using this relation, we have from (A4)

$$\frac{\partial}{\partial L}E\{\tau_3^2\}=8a^2a_\omega^2L-6a^2E\{\tau_3^2\} \tag{A6}$$

which gives

$$E\{\tau_3^2\}=\frac{4}{3}a_\omega^2L-\frac{2a_\omega^2}{9a^2}+\frac{2a_\omega^2}{9a^2}\exp\left(-6a^2L\right). \tag{A7}$$

Inserting (A7) into (A2) and (A3), we find

$$E\{\tau_1^2\}=E\{\tau_2^2\}=\frac{4}{3}a_\omega^2L+\frac{a_\omega^2}{9a^2}-\frac{a_\omega^2}{9a^2}\exp\left(-6a^2L\right). \tag{A8}$$

The second terms of (A7) and (A8) represent residual couplings between n=0 mode and higher-order modes.

In a similar way, applying $\partial^2/\partial k_{\omega i}^2$ to (16) and setting $\boldsymbol{k}=\boldsymbol{k}_\omega=0$, we find

$$\frac{\partial}{\partial L}E\{\tau_{\omega1}^2\}=-2a^2\left(E\{\tau_{\omega1}^2\}-E\{\tau_{\omega3}^2\}\right)+2a_\omega^2E\{\tau_3^2\}-4aa_\omega\left(E\{\tau_1\tau_{\omega1}\}-E\{\tau_3\tau_{\omega3}\}\right)+2a_{\omega\omega}^2. \tag{A9}$$

$$\frac{\partial}{\partial L}E\{\tau_{\omega2}^2\}=-2a^2\left(E\{\tau_{\omega2}^2\}-E\{\tau_{\omega3}^2\}\right)+2a_\omega^2E\{\tau_3^2\}-4aa_\omega\left(E\{\tau_2\tau_{\omega2}\}-E\{\tau_3\tau_{\omega3}\}\right)+2a_{\omega\omega}^2 \tag{A10}$$

$$\begin{aligned}\frac{\partial}{\partial L}E\{\tau_{\omega3}^2\}&=2a^2\left(E\{\tau_{\omega1}^2\}+E\{\tau_{\omega2}^2\}\right)-4a^2E\{\tau_{\omega3}^2\}\\&+4aa_\omega\left(E\{\tau_1\tau_{\omega1}\}+E\{\tau_2\tau_{\omega2}\}-2E\{\tau_3\tau_{\omega3}\}\right)\\&+2a_\omega^2\left(E\{\tau_1^2\}+E\{\tau_2^2\}\right)\end{aligned} \tag{A11}$$

Adding these three equations, we have

$$\frac{\partial}{\partial L}E\{\tau_\omega^2\}=2a_\omega^2\left(E\{\tau_1^2\}+E\{\tau_2^2\}+2E\{\tau_3^2\}\right)+4a_{\omega\omega}^2 \tag{A12}$$

$$=\frac{32}{3}a_\omega^4L+4a_{\omega\omega}^2-\frac{4a_\omega^4}{9a^2}+\frac{4a_\omega^4}{9a^2}\exp\left(-6a^2L\right) \tag{A13}$$

$$E\{\tau_\omega^2\}=\frac{16}{3}a_\omega^4L^2+4L\left(a_{\omega\omega}^2-\frac{a_\omega^4}{9a^2}\right)+\frac{2a_\omega^4}{27a^4}\{1-\exp\left(-6a^2L\right)\} \tag{A14}$$

Applying the relation, $E\{\tau^2\}=-\nabla_k^2Q(\boldsymbol{k},\boldsymbol{k}_\omega,L)|_{k=k_\omega=0}$, to (35) directly, we find $E\{\tau^2\}=4a_\omega^2L$. Also, $E\{\tau_\omega^2\}$ is found from (35) as $16a_\omega^4L^2/3+4a_{\omega\omega}^2L$. The second term is slightly different from the exact expression, (A14). This is because (35) neglects higher order modes with $L_{tot}\neq0$.

APPENDIX B

This Appendix illustrates that the $a_{\omega\omega}$ term can be meaningful for practical transmission distances. We concentrate on $Q(0,\boldsymbol{k}_\omega,L)$, the 3-dimensional Fourier transform of $\boldsymbol{\tau}_\omega$ vector's pdf. It has the following form:

$$Q(0,\boldsymbol{k}_\omega,L)=\frac{\exp\left(-a_{\omega\omega}^2k_\omega^2\sigma^2/2a_\omega^2\right)}{\cosh\left(k_\omega\sigma^2\right)} \tag{B1}$$

$$=\frac{\exp\left\{-\eta\left(k_\omega\sigma^2\right)^2\right\}}{\cosh\left(k_\omega\sigma^2\right)} \tag{B2}$$

where $\eta\equiv a_{\omega\omega}^2/2a_\omega^2\sigma^2$. Note that η is inversely proportional to L. Thus the soliton shape, $1/\cosh\left(k_\omega\sigma^2\right)$, is obtained at $L=\infty$ [2]. On the other hand, when η is sufficiently large, the denominator is almost fixed to 1 for the appreciable region of the numerator. Then $Q(0,\boldsymbol{k}_\omega,L)$ can be approximated as a Gaussian, $\exp\left\{-\eta\left(k_\omega\sigma^2\right)^2\right\}$, and each component of $\boldsymbol{\tau}_\omega$ also becomes a Gaussian process. The magnitude of $\boldsymbol{\tau}_\omega$, in this case, resembles a Maxwellian distribution.

We plot in Fig. B1 $Q(0,\boldsymbol{k}_\omega,L)$ versus $k_\omega\sigma^2$ for several values of η. The η= 0 curve is the soliton shape obtained when $L=\infty$ or when $a_{\omega\omega}$=0. If the transmission distance is finite, the evolution of $Q(0,\boldsymbol{k}_\omega,L)$ is dependent on the ratio, $a_{\omega\omega}/a_\omega$, within η. The ratio can be found from $(\partial\tau_{rms}/\partial\omega)/\tau_{rms}$, where $\tau_{rms}\equiv\sqrt{E\{\tau^2\}}=2a_\omega\sqrt{L}$. This value is

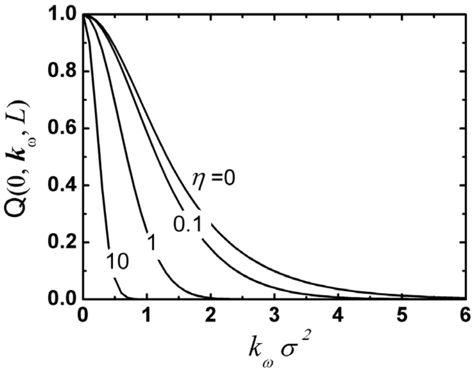

FIG. B1. Plot of $Q(0,\boldsymbol{k}_\omega,L)$ versus $k_\omega\sigma^2$ for several values of η. The η=0 line is obtained when $L=\infty$ or when $a_{\omega\omega}$=0.

distributed roughly as -20 ps $\le a_{\omega\omega}/a_\omega \le$ 20 ps [2]. For example, when $a_{\omega\omega}/a_\omega$ is 1 ps and a_ω=0.01735 $\mathrm{ps}/\sqrt{\mathrm{km}}$ [12], we have η=10 for L= 124 km, where $Q(0,\boldsymbol{k}_\omega,L)$ is much like a Gaussian rather than the soliton shape. When $a_{\omega\omega}/a_\omega$ is 10 ps, we have η=10 for L as large as 12,400 km.

ACKNOWLEDGMENT

This work was partly supported by National Research Foundation of Korea Grant funded by the Korean Government (KRF-2007-313-D00550) and also partly supported by the Research Grant of Kwangwoon University in 2010.

REFERENCES

1. C. D. Poole and J. Nagel, “Polarization effects in lightwave systems,” in *Optical Fiber Telecommunications III-A,* I. P. Kaminow and T. L. Koch, eds. (Academic, San Diego, CA, USA, 1997), Chapter 6.
2. H. Kogelnik and R. M. Jopson, “Polarization-mode dispersion,” in *Optical Fiber Telecommunications IVB Systems and Impairments,* I. P. Kaminow and T. Li, eds. (Academic, San Diego, CA, USA, 2002), Chapter 15.
3. H. Jang, K. Kim, J. Lee, and J. Jeong, “Theoretical investigation of first-order and second-order polarization-mode dispersion tolerance on various modulation formats in 40 Gb/s transmission systems with FEC coding,” J. Opt. Soc. Korea **13**, 227-233 (2009).
4. G. J. Foschini and L. A. Shepp, “Closed form characteristic functions for certain random variables related to Brownian motion,” in *Stochastic Analysis*, *Liber Amicorum for Moshe Zakai* (Academic, New York, USA, 1991), pp. 169-187.
5. G. J. Foschini and C. D. Poole, “Statistical theory of polarization dispersion in single mode fibers,” IEEE J. Lightwave Technol. **9**, 1439-1456 (1991).
6. G. J. Foschini, R. M. Jopson, L. E. Nelson, and H. Kogelnik, “The statistics of PMD-induced chromatic fiber dispersion,” IEEE J. Lightwave Technol. **17**, 1560-1565 (1999).
7. G. J. Foschini, L. E. Nelson, R. M. Jopson, and H. Kogelnik, “Probability densities of second-order polarization mode dispersion including polarization dependent chromatic fiber dispersion,” IEEE Photon. Technol. Lett. **12**, 293-295 (2000).
8. G. J. Foschini, L. E. Nelson, R. M. Jopson, and H. Kogelnik, “Statistics of second-order PMD depolarization,” IEEE J. Lightwave Technol. **19**, 1882-1886 (2001).
9. J. P. Gordon, “Statistical properties of polarization mode dispersion,” in *Polarization Mode Dispersion*, A. Galtarossa and C. R. Menyuk, eds. (Springer, New York, USA, 2005), pp. 52-59.
10. A. Galtarossa and L. Palmieri, “Measure of twist-induced circular birefringence in long single-mode fibers: theory and experiments,” IEEE J. Lightwave Technol. **20**, 1149-1159 (2002).
11. H. Risken, *The Fokker-planck Equation Methods of Solution and Applications*, 2nd ed. (Springer-Verlag, New York, USA, 1996), Chapter 3, pp. 54-56.
12. J. S. Lee, “Analysis of the polarization-mode-dispersion vector distribution for linearly birefringent optical fibers,” IEEE Photon. Technol. Lett. **19**, 972-974 (2007).
13. J. S. Lee, “Derivation of the Foschini and Shepp’s joint-characteristic function for the first-and second-order polarization-mode-dispersion vectors using the Fokker-Planck method,” J. Opt. Soc. Korea **12**, 240-243 (2008).
14. G. B. Arfken and H. J. Weber, *Mathematical Methods for Physicists*, 6th ed. (Elsevier Academic, New York, USA, 2005), p. 130.
15. Y. Tan, J. Yang, W. L. Kath, and C. M. Menyuk, “Transient evolution of the polarization-dispersion vector’s probability distribution,” J. Opt. Soc. Am. B **19**, 992-1000 (2002).
16. G. B. Arfken and H. J. Weber, *Mathematical Methods for Physicists*, 6th ed. (Elsevier Academic, New York, USA, 2005), Chapter 4.